**UNIVERSITÀ DEGLI STUDI DI BERGAMO**
**DIPARTIMENTO DI INGEGNERIA DELL'INFORMAZIONE**
**E METODI MATEMATICI**°

**QUADERNI DEL DIPARTIMENTO**

**Department of Information Technology and Mathematical Methods**

**Working Paper**

**Series "*Mathematics and Statistics*"**

n. 6/MS – 2009

# *Computational Fluid Dynamics-based estimation of blood flow rate in Doppler analysis: In vivo validation by means of Phase Contrast Magnetic Resonance Imaging*

by

**R. Ponzini, C. Vergara, G. Rizzo, A. Veneziani,**
**A. Redaelli, A. Roghi, A. Vanzulli, O. Parodi**

° Viale Marconi. 5, I – 24044 Dalmine (BG), ITALY, Tel. +39-035-2052339; Fax. +39-035-562779

[§] L'accesso alle *Series* è approvato dal Comitato di Redazione. I *Working Papers* della Collana dei Quaderni del Dipartimento di Ingegneria dell'Informazione e Metodi Matematici costituiscono un servizio atto a fornire la tempestiva divulgazione dei risultati dell'attività di ricerca, siano essi in forma provvisoria o definitiva.

**Full title**: Computational Fluid Dynamics-based estimation of blood flow rate in Doppler analysis: *In vivo* validation by means of Phase Contrast Magnetic Resonance Imaging

**Authors:**

- Raffaele Ponzini, Ph.D., CILEA, Segrate (MI), Italy
- Christian Vergara, Ph.D., Department of Information Engineering and Mathematical Methods, Università degli Studi di Bergamo, Italy
- Giovanna Rizzo, Eng., Institute of Molecular Bioimaging and Physiology, CNR, Italy
- Alessandro Veneziani, Ph.D., Department of Mathematics and Computer Science, Emory University and Wallace H Coulter Department of Biomedical Engineering at Georgia Tech and Emory, Atlanta USA
- Alberto Redaelli, Ph.D., Department of Bioengineering, Politecnico di Milano, Italy
- Alberto Roghi, MD, Ca' Granda Niguarda Hospital, Milano, Italy
- Angelo Vanzulli, MD, Ca' Granda Niguarda Hospital, Milano, Italy
- Oberdan Parodi, MD, Institute of Clinical Physiology CNR, Pisa, Italy and Ca' Granda Niguarda Hospital, Milano, Italy

**Short title:** *In vivo* validation of CFD-based estimates of flow.

**Correspondance**: Alessandro Veneziani, Department of Mathematics and Computer Science Emory University Mathematics and Science Center, Room N418 Atlanta, GA 30322, USA Phone: +1 404 727 7925 Fax : +1 404 727 5611

**Abstract:**

We carry out an *in vivo* validation of a new method for estimating blood flow rate from the maximum velocity, as it is usually done in single-wire Doppler catheter measurements**.** A common practice is to measure the centerline velocity and to recover the flow rate (*a-priori* approach) by exploiting an assumption on the shape of velocity profile, either a parabolic or a flat one,. Our method proposes a new formula valid for the peak instant linking the maximum velocity and the flow rate including the Womersley number, in order to account in a more accurate way the haemodynamics conditions (*Womersley-based* approach).

*In vivo* validation of the *Womersley-based* approach is performed. An experimental protocol using cine Phase Contrast MRI (2D PCMRI) technique has been designed and applied to ten healthy young volunteers in three different arterial districts: the abdominal aorta, the common carotid artery and the brachial artery. Each PCMRI dataset has been used twice. 1) To compute the value of the blood flow rate used as a gold standard. 2) To estimate the flow rate using information only on the maximum velocity and on the diameter value (i.e. emulating the intravascular Doppler data acquisition) by using the *a priori* and the *Womersley-based* approaches.

All the *in vivo* results concerning the three arterial districts allow to state that the Womersley-based approach provides better estimates of the flow rate at the peak instant with the respect to the *a-priori* approach. These results might have relevant clinical implication, for example in *Coronary Flow Reserve* determination.

**Keywords:** Blood flow, Doppler estimate, Womersley number

## Introduction

Measurement of the maximum velocity $V_M$ over a cross-section using a single-point Doppler based instrumentation to estimate the value of the flow rate $Q$ is a common clinical practice in intravascular blood flow analysis. Knowledge of $Q$ is in fact an indicator of the correct perfusion of tissues, for grading artery stenosis and then supporting decisions on surgical interventions. During single point intravascular Doppler velocimetry analysis, when the acquisition procedure can be performed in sites sufficiently far from branching, bending and strongly tapered regions (*cylindrical symmetry hypothesis*), it is usually assumed that the flow rate can be obtained from the maximum velocity $V_M$, making an *a priori* assumption on the velocity profile. This approach – hereafter referred to as *a priori approach* - has been validated for time-averaged blood flow rate estimation in the coronaries (see [8]). Successively, it has been applied to a wide range of vascular districts (see, e.g., [28, 15, 37, 34, 35, 45]) and under very different blood flow conditions (e.g., baseline, atrial pacing, see, e.g., [20, 19]) and also for peak velocity instant flow rate estimate (see, e.g, [39]).

Within this approach there are two kinds of spatial velocity profiles that are usually considered, namely *parabolic* and *flat ones* . Nevertheless, the shape of the spatial velocity profile is not known *a priori* (see, e.g., [17-18]). Indeed, it is known that the shape of the velocity profile is influenced by many factors, including pulsatility, viscosity and diameter of vascular districts (see [46, 25, 38]). For this reason, the *a priori* approach could lead to inaccurate estimates (see, e.g., [17,18,33]).

A new approach for the estimation of the flow rate at the peak instant has been proposed in [33]. This strategy stems from the application of a Computational Fluid Dynamics (CFD) technique, where the flow rate is prescribed through the introduction of a Lagrange multiplier (see [42]). Starting from the data arising from a set of simulations performed with this technique, a new

formula linking the maximum velocity and the peak flow rate has been proposed. This can be considered as a generalization of the *a priori* method and it is based on the assumption that the relationship between flow rate and maximum velocity at the peak instant can be better established by taking into account the haemodynamics conditions by means of the Womersley number, which depends on the heart pulsatility, the blood viscosity and the vessel diameter. For this reason, in what follows, this method will be referred as *Womersley-based* approach (see Appendix for details).

In [33] and [32] this method has been validated *in silico* in realistic geometries, whilst in [43] it has been applied to a clinical dataset. In this paper, we present the first *ad hoc in vivo* validation of the Womersley-based approach, based on a 2D cine phase contrast MRI data processing, as suggested in [31], with the aim of highlighting the performances of the new approach by showing that the velocity profiles in humans could be far from parabolic or flat.

## Material and methods

*Phase contrast MRI : acquisition procedure*

Ten healthy young volunteers (with age varying between 25-42 years, weight 60-95 kg, all males) have been acquired under baseline conditions using a cine phase contrast MRI protocol for a total scan duration equal to 40 minutes. All the volunteers signed an informed consent according to the ethic institutional review board of the Niguarda Ca' Granda Hospital (Milan, Italy). Arterial pressure were measured before the acquisition and after the overall protocol to ensure stable haemodynamics conditions and parameters. The baseline measurements have been acquired leaving the subject in resting condition before entering in the MRI chamber for a sufficient amount of time (about five minutes). The heart rate has been continuously monitored along all the acquisition by means of the ECG device used in the PCMRI cardiac gating instrumentation.

*Phase contrast MRI : study design*

We have considered three anatomical sites with different cross section area and located at different levels of the arterial tree, sampling most of the physiological range of the Womersley number in humans. Moreover, we excluded branching or strongly tapered sites, so that assumptions behind the *a priori* approach (i.e. *the cylindrical symmetry hypothesis*) are satisfied. More precisely, *the brachial artery, the common carotid artery* and *the descending aorta* have been chosen to represent small, medium and large vessels, respectively. Figure 1 shows samples of the three anatomical sites in one representative volunteer. For each volunteer we acquired the abdominal aorta and common carotid data under supine position, while the brachial artery data have been acquired under prone position to ensure maximum stability and comfort and an optimal centring in the main magnetic field accordingly to the MR technician experience. On each arterial district the scan acquisition took about ten minutes.

*Phase contrast MRI : instrumentation and parameters*

Two-dimensional Phase Contrast data have been acquired using an MR Siemens Magnetom Avanto 1.5 T scanner equipped with a 12-channel cardiac phased-array coil and with gradient of maximum intensity equal to 45mT /m and slew rate equal to 200T/m/s. The pulse sequence for 2D CINE PCMRI data acquisition was a T1-weighted cardiac-gated (retrospective gating) with velocity encoding along the direction orthogonal to the slice orientation ("through-plane" encoding). The region of interest (ROI) was centred as much as possible within the field of view (FOV). Flip angle was set to 30°. Other parameter sequences such as the repetition time (TR) and the time to echo (TE) as well as image spatial and temporal resolution have been adapted for the different vessels in order to preserve a detailed in plane spatial accuracy and assuming constant the total scan time. In particular, the in plane pixel values ranges from 0.4 mm to 1 mm according to the different size of the vascular districts. More precisely in Table 1 the settings for each arterial districts is shown in

term of repetition time (TR), time to echo (TE), pixel size, slice thickness and number of cardiac phases.

For each subject and in each district, a preliminary encoding velocity scout sequence has been performed for optimizing the value of such velocity, $V_{enc}$, out of three possible values. This preliminary sequence allowed us to avoid any aliasing artefacts in the final phase image.

*Phase contrast MRI : image processing and validation protocol*

In the present work a semi-automatic method proposed in [1] has been used to segment the phase images and extract wall vessels directly from the velocity field image. After the segmentation process, we performed a further processing of the images as shown in Figure 2, where the overall flow chart of the validation protocol is presented. At the peak velocity instant the processed PCMRI images have been used in two ways.

a) The maximum velocity $V_M$ and the diameter $D$ of the section at hand have been used for estimating the flow rate $Q$ at the peak instant through this section, mimicking the intravascular Doppler analysis. In particular, we compute both the *a priori* estimate ($Q_A$) and the Womersley-based one ($Q_W$). We will call these values *estimated flow rates*.

b) The entire spatial velocity profile has been used for retrieving an accurate flow rate measure by means of (numerical) integration over the artery cross section area. This has been used as gold standard value ($Q_{GS}$), denoted as *computed flow rate*.

*MRI-based and Doppler-like estimates*

Operatively, the gold standard value $Q_{GS}$ of the blood flow rate has been computed by numerical integration of the local velocity field $V_{pi}$ taken on each pixel *pi* of the lumen. More precisely, we set:

$$Q_{GS} \equiv \sum_{pi} V_{pi} \times A_{pi} \qquad (1)$$

where $A_{pi}$ is the area of the single intra-vessel pixel *pi*.

On the other hand the estimate procedure is performed in all the considered cases following the two different approaches. In particular, the *a priori* approach consists in the following equation:

$$\mathrm{Q_A} = k_A \times V_M \times \sum_{pi} A_{pi} \qquad (2)$$

where

$k_A = 0.5$ for parabolic profile
$k_A = 1$ for flat profile

whilst the 'Womersley-based' approach, reads:

$$Q_W = k_W \times V_M \times \sum_{pi} A_{pi} \qquad (3)$$

where $k_W$ depends on the Womersley number $W$ and is defined in the Appendix.

For all the estimations in the subjects, a constant values of blood viscosity (0.035 Poise) and density (1.060 g/cm$^3$) have been assumed, accordingly to the fact that all the volunteers where healthy subjects.

*Statistical analysis*

The Bland-Altman test is a clinical indicator of the equivalence of two different measure procedures for the same quantity and it has been proved to able to quantify their correlations [3]. Here the Bland-Altman test has been performed in order to establish the reliability of the two estimates approaches (namely the *a priori* and the Womersley-based). In particular, the two estimates ($Q_A$ and $Q_W$) have been compared to the reference value $Q_{GS}$.

The authors have full access to data and take responsibility for their integrity. All authors have read the manuscript as written and agree with it.

## Results

The values of the estimated flow rates at the peak instant ($Q_A$ and $Q_W$, eqns. (2) and (3)) have been compared to their associated gold standard values $Q_{GS}$ (eqn. (1)) for a total of 30 observations (three district for ten volunteers), covering a range of the Womersley number between 2.5 and 14.7. We point out that we use the flat assumption only for the dataset collected in the abdominal aorta where a parabolic hypothesis is known to be unreliable and a flat profile is commonly hypothesized.

*Blood flow velocity measurements and flow rate estimates*

In Figure 3 we summarize the measures of interest for the purposes of this analysis, namely vessel diameter ($D$ in cm), maximum velocity ($V_M$ in cm/s), heart rate (HR in beat/min), Womersley number $W$ and gold standard flow rate ($Q_{GS}$ in $cm^3/s$). The three districts clearly feature separated values of $D$ , $V_M$ , $W$ and $Q_{GS}$, as highlighted by their mean values.

In Figure 4 the estimated flow rates $Q_A$ and $Q_W$ (eqn. (2) and (3)) together with the gold standard $Q_{GS}$ (eqn. (1)) are shown.

*Statistical analisys*

In Figure 5 we report for the two approaches a synthesis of the percentage differences, in terms of mean value and variance, in the three arterial districts.

In Figure 6 we report the result of the Bland-Altman test [3]. On the horizontal axis we report the average between the gold standard and the estimated flow rates, on the vertical axis we report their differences. The solid line indicates the mean values of the differences, the dashed one the variance. The results obtained with the *a priori* and with the Womersley-based approaches are shown in the left and in the right panel, respectively.

*Visualization of spatial velocity profiles*

To get a visualization of the spatial velocity profile present in the three studied districts at the peak velocity instant, in Figure 7 we report the three-dimensional (3D) spatial velocity profiles for three subjects. In order to get a clearer representation, for one selected subject, we compare the acquired velocity profile across a single diameter (2D) with the corresponding parabolic (flat for the abdominal aorta) profile, featuring the same value of the centreline velocity.

## Discussion

*Phase contrast MRI : motivations*

Let us discuss the appropriateness of the Phase contrast MRI in the context of this validation. 2D cine PCMRI is a suitable, accurate tool to acquire blood flow rate in human arteries. Moreover within the same measurement procedure it is able to provide both geometrical and fluid dynamics data, namely the maximum velocity, the diameter and the heart rate [13, 23, 6, 22, 2, 5, 7, 41, 9, 26, 24]. This technique provides non invasively a rich dataset where the space and time resolution of the blood velocity within the cross section areas at hand is sufficient to perform local haemodynamics characterization (see [44, 11, 40, 4, 10, 30, 16, 14, 29, 12, 27]). The advantages of this approach are that:

- All the measures are performed at the same time and at the same position;
- No external devices or contrast agent that can potentially alter the blood flow (e.g.. *Intravascular Ultrasound* (IVUS) or intravascular Doppler tips) are introduced within the vessel;
- The MRI scan procedure allows to accurately check the sampling plane within the vascular anatomy and to easily position it far from region with branches or bends;
- Spatial accuracy of sampling is easily adapted to the different districts.

For these reasons, we consider PCMRI adequate for our *in vivo* validation of Doppler derived blood flow rate estimates and we design a suitable protocol for the acquisition procedures in order to mimic Doppler-like analysis with a gold-standard reference based on all the spatial PCMRI dataset.

*Data requirements*

For the application of the Womersley-based approach, only the measurement of the vessel diameter, of the viscosity and of the maximum velocity are needed. Therefore, this strategy does not require any new data with respect to those already acquired during a typical Doppler analysis (see [33, 31, 32, 43]). The application of formula (3) is therefore immediate in practice. Indeed, in [43] this approach has been applied, without any new acquisition, to a velocimetry Doppler dataset to provide a *Coronary Flow Reserve* (CFR) evaluation.

*Blood rheology*

The viscosity of blood has been considered to be constant for all subjects. This hypothesis is justified by theoretical and clinical observations, as discussed in [43], where it has been shown the negligible dependence of the flow rate estimate on the rheology model.

*Doppler-like analysis: blood flow rate estimates and spatial velocity profiles*

The results reported in Figure 4 clearly show that the Womersley-based approach better estimates the flow rate with the respect to the *a priori* approach in all the 30 evaluations. In particular, the *a priori* approach leads to a systematic underestimation or overestimation of the flow rate for the parabolic and flat assumptions respectively. For example, the *a priori* approach in medium and small sized vessels (diameter values between 0.38 and 0.74 cm in our dataset – parabolic approximation) is affected by an error of about 16%, while the Womersley-based one features about 3.7%.

The mean performances of the two approaches (Fig. 5) confirm that the Womersley-based approach is able to provide remarkably better performances. The statistical analysis provided by the Bland-Altman method (Fig. 6) also confirms that the Womersley-based approach is more reliable than the *a priori* approach. Indeed, the absolute value of the mean error is clearly lower with a smaller variance (8.2 ± 28.3 $cm^3/s$ for the Womersley based vs -19.1 ± 61.4 $cm^3/s$ for the *a priori* one).

As a matter of fact, the assumptions behind the *a priori* approach are unreliable as shown by the visualization of the three-dimensional spatial velocity profiles at the peak velocity instant (Fig. 7). In the same figure, we compare also the acquired velocity profile across a single diameter with the corresponding parabolic (or flat for the abdominal aorta) profile, featuring the same value of the centreline velocity. Even if *cylindrical symmetry hypothesis* is quite acceptable, velocity profiles assumed in the *a priori* approach are pretty inaccurate.

*Dependence of the error on W*

In Figure 8, left, the relative error, with respect to the gold standard value, is reported as function of the Womersley number for the two estimates. Considering the overall trend of the *a priori* approach we observe that the error seems to become higher as the values of *W* increases. On the contrary, the intrinsic dependence of the novel proposed approach on *W* (i.e. on the vessel diameter, blood viscosity and on the heart pulsatility) enables the corresponding flow estimates to account for these features in the various vascular districts and under different heart rate conditions.

*CFD vs in vivo dataset acquisition*

In [33] the performances of the *a priori* approach have been analyzed with an *in silico* validation. In particular, numerical simulations in cylindrical domains prescribing at the inlet the flow rate through the introduction of a Lagrange multiplier (see [42]) have been performed. The flow rates

obtained by the maximum velocities at the inlet making the parabolic assumption have been compared with the prescribed flow rates, used as gold standard in that case.

In Fig. 8, right, we compare the relative errors, as function of the Womersley number, obtained by using the *a priori* approach, in the *in silico* validation in [33], with those obtained in the present *in vivo* validation. We point out that the order of magnitude of the errors is close in the two cases for a fixed value of the Womersley number. This agreement confirms the reliability of the strategy proposed in [42] for the prescription of the flow rate and the effectiveness on one hand of CFD as complementary environment for fast and unexpensive data acquisition (with the respect to the more traditional *in vivo* and *in vitro* ones).

*Possible clinical applications*

Womersley number depends on the diameter, on the heart rate and on the viscosity. In the present work, the viscosity is assumed to be constant among all the subjects, while the diameter varies in the range 1.0 +/- 0.65 cm, and the heart rate in 56.8 +/- 6.2 bpm. Therefore, in the results presented in the previous section, the variation on the shape of the spatial velocity profile is due mainly to the variability of the diameter. In particular, the results reported in Figure 4 and in Figure 8 (left) show that the error of the *a priori* approach gets higher when $D$ (and then $W$) increases, whilst with the Womersley-based approach they are confined below 15.75%. Therefore, we can state that the *a priori* approach is in particular not recommended in medium and large vessels.

However, it is known that the shape of the velocity profiles depends also on the heart rate (see [45] for a theoretical discussion). Therefore, we expect that the *a priori* approach is not able to catch this dependence, since it assumes the shape of the velocity profile independently of the cardiac frequency. On the contrary, the dependence of eqn. (3) on the Womersley number (and consequently on the heart rate), allows us to state that the Womersley-based approach can provide significant better estimates of the flow rate, also for higher heart rates. This could have relevant clinical implications. For example, a correct estimation of CFR is central in interventional clinics,

since it has been extensively used to assess coronary vasodilating capability in patients with suspected or known coronary artery disease (CAD) (see [36]). This goal is achieved by estimating coronary flow rate in resting conditions and during increases in myocardial oxygen demand by exercise, atrial pacing, dobutamine infusion, or during coronary vasodilatation, such as following adenosine or dipyridamole infusion (see [21]) being all these stressors responsible for increases in heart rates.

**Limitations and conclusions**

There are several limitations and possible extensions to the present work.

i) The value of $V_M$ has been obtained still using PCMRI. Obviously, a more effective comparison between the different estimated flow rates could be performed by acquiring the value of $V_M$ with a Doppler technique. However, this would introduce a bias in the two measurements due to possible different physiological conditions of the subject during the two acquisitions that could not be acquired at the same instant. For this reason, we decide to process the value of $V_M$ acquired with the PCMRI, yielding the gold standard computations and the estimates from measures acquired at the same time.

ii) The PCMRI measures are known to underestimate the 'true' value of the $V_M$. In general, PCMRI evaluations get higher accuracy when performed with high spatial and temporal resolution like in our protocol (see [30, 12]). The gold standard flow rate computation depends on the area detection *on* the phase images. As pointed out in the Materials and Methods Section we resorted to a robust segmentation method, guaranteeing a good level of operator independence. It is worth observing that the *in silico* validation provided in [33] actually gave similar results when gold standard were provided by "exact" numerical values (i.e. analytically determined). A possible further step for reducing uncertainty from gold standard values is to resort to an *in vitro* validation using MRI pulsatile flow phantoms.

iii) Our investigation does not sample values in the interval of the Womersley number between 5.9 and 11.8. Unfortunately this was not under the control of the authors, since all the acquisition have been done under baseline conditions and then without the possibility to modify the heart rate over the physiological inter-subject variability to fill out all the range of $W$.

Despite of these limitations and possible improvements, the present study confirms after *in vivo* validation that the new Womersley-based method for estimating blood flow from the measurement of $V_M$ is by far better than the traditional ones at the same cost, i.e. without requiring any different or new procedures. The key-point is the consideration of the haemodynamics conditions by the inclusion of the Womersley number in the flow rate estimation, which automatically improves the reliability of the procedure.

It is finally worth to mention that Womersley-based method is the result of a statistical analysis conducted over hundreds of numerical simulations performed in [33]. The reliability of this approach can be therefore further improved in three ways.

i) Set up of parameters of eqn. (3) can be improved by including more numerical simulations in the statistical analysis.

ii) Equation (3) has been devised with a "general purpose" perspective, i.e. covering a wide (physiological) range of Womersley number. If the Womersley numbers of interest refer to a limited interval, an *ad hoc* formula can be devised with the same procedure, so that in the range of interest flow rate estimations can be further enhanced (see [33]).

iii) The approach could be extended to the whole cardiac cycle, this would require to include the sampling of the maximum velocity over the cardiac cycle thus allowing an estimate of the mean flow rate.

**Appendix**

The flow rate through a section $\Gamma$ is defined as

$$Q = \rho \int_{\Gamma} u \cdot n d\gamma$$

Where $u$ is the blood velocity, $\rho$ is the blood density assumed constant and $n$ the normal unit vector. In order to obtain $Q$ the whole spatial velocity profile is needed. However, the flow rate can be approximated by the formula

$$Q = k \times V_M \times A$$

for a suitable value of $k$. For example, in a cylinder in steady conditions, we have $k=0.5$ (parabolic profile). However, this value is not correct for not cylindrical domains (even if the *cylindrical symmetry hypothesis* is satisfied) and in pulsatile conditions. For this reason, other values of $k$ need to be found in order to get a better estimate of the flow rate. For example, in large vessel for high values of the Reynolds number, it is a common practice to use the value $k=1$ (flat profile). However, this *a priori* choice of $k$ is not satisfactory in the general case. For this reason, in [33] it has been proposed the following expression

$$k=k_W=\begin{cases} g_1 & W \le 2.7 \\ p \times g_1 + (1-p) \times g_2 & 2.7 < W \le 3.1 \\ g_2 & 3.1 < W \le 15. \end{cases} \qquad (3)$$

where $g_1(W) = \frac{1}{2} \times (1 + a_1 W^{b1})$; $\quad g_2(W) = \frac{1}{2} \times b_2 \arctan(a_2 W)$;

$$\begin{cases} a_1 = 0.00417, & b_1 = 2.95272 \\ a_2 = 1.00241, & b_2 = 0.94973 \end{cases} \quad \text{and} \quad p = e^{\frac{W-2.7}{(W-2.7)-(3.1-2.7)}}$$

and $W$ is the Womersley number

$$W = D\sqrt{f\pi/(2\nu)}$$

with $f$ the heart rate and $\nu$ the blood viscosity.

**Acknowledgments**

C. Vergara wishes to thank the Staff of the Math & CS Department of Emory University for the nice hospitality and fruitful environment in preparing this work.

**References**

[1] Alperin N, Lee SH. PUBS: Pulsatility-Based Segmentation of Lumens Conducting Non-steady Flow. Mag. Res. Med., 49(5):934-44, 2003.

[2] Axel L. Blood flow effects in magnetic resonance imaging. AJR Am J Roentgenol., 143: 1157–1166, 1984.

[3] Bland J.M., Altman D.G., Statistical methods for assessing agreement between two methods of clinical measurement. Lancet., 1(8476):307-310, 1986.

[4] Bogren HG, Underwood SR, Firmin DN, et al. Magnetic resonance velocity mapping in aortic dissection. Br J Radiol., 61:456–462, 1988.

[5] Bryant DJ, Payne JA, Firmin DN, Longmore DB. Measurement of flow with NMR imaging using a gradient pulse and phase difference technique. J Comput Assist Tomogr., 8:588–593, 1984.

[6] Burt CT. NMR measurements and flow. J Nucl Med., 23:1044–1045, 1982.

[7] Constantinesco A, Mallet JJ, Bonmartin A, Lallot C, Briguet A. Spatial or flow velocity phase encoding gradients in NMR imaging. Magn Reson Imaging., 2:335–340, 1984.

[8] Doucette JW, Corl PD, Payne HM, Flynn AE, Goto M, Nassi M, Segal J. Validation of a Doppler guide wire for intravascular measurement of coronary artery flow velocity. Circulation., 85, 1899-1911, 1992.

[9] Feinberg DA, Crooks LE, Sheldon P, Hoenninger J 3rd, Watts J, Arakawa M. Magnetic resonance imaging the velocity vector components of fluid flow. Magn Reson Med., 2:555–566, 1985.

[10] Firmin DN, Nayler GL, Kilner PJ, Longmore DB. The application of phase shifts in NMR for flow measurement. Magn Reson Med., 14:230–241, 1990.

[11] Firmin DN, Nayler GL, Klipstein RH, Underwood SR, Rees RS, Longmore DB. In vivo validation of MR velocity imaging. J Comput Assist Tomogr., 11:751–756, 1987.

[12] Frayne R, Steinman DA, Ethier CR, Rutt BK. Accuracy of MR phase contrast velocity measurements for unsteady flow. J Magn Reson Imaging., 5:428–431, 1995.

[13] Hahn EL. Detection of sea water motion by nuclear precession. J Geophys Res., 65(2): 776–777, 1960.

[14] Hangiandreou NJ, Rossman PJ, Riederer SJ. Analysis of MR phase-contrast measurements of pulsatile velocity waveforms. J Magn Reson Imaging., 3:387–394, 1993.

[15] Kamata T, Moriuchi M, Saito S, Takaiwa Y, Horiuchi K, Takayama T, Yajima J, Shimizu T, Honye J, Tanigawa N, Ozawa Y, Kanmatsuse K. Measurement of pulmonary artery flow velocity using a Doppler guidewire. Japanese Journal of Interventional Cardiology., 11 (2): 31-37, 1996.

[16] Kraft KA, Fei DY, Fatouros PP. Quantitative phase-velocity MR imaging of in-plane laminar flow: effect of fluid velocity, vessel diameter, and slice thickness. Med Phys., 19:79–85, 1992.

[17] Jenni R, Kaufmann PA, Jiang Z, Attenhofer C, Linka A, Mandinov L. In vitro validation of volumetric blood flow measurement using doppler flow wire. Ultrasound in Medicine \& Biology., 26(8):1301-10, 2000.

[18] Jenni R, Matthews F, Aschkenasy SV, Lachat M, van Der~Loo B, Oechslin E, Namdar M, Jiang Z, Kaufmann PA. A novel in vivo procedure for volumetric flow measurements. Ultrasound in Medicine \& Biology., 30(5):633-7, 2004.

[19] Johnson EL, Yock PG, Hargrave VK, Srebro JP, Manubens SM, Seitz W, Ports TA. Assessment of severity of coronary stenoses using a doppler catheter. validation of a method based on the continuity equation. Circulation., 80(3):625-35, 1989.

[20] Iliceto S., Marangelli V., Memmola C., Rizzon P. Transesophageal doppler echocardiography evaluation of coronaryblood flow velocity in baseline conditions and during dipyridamole-induced coronary vasodilation. Circulation., 83(1):61-9, 1991.

[21] McGinn AL, White CW, Wilson RF. Interstudy variability of coronary flow reserve. Influence of heart rate, arterial pressure, and ventricular preload. Circulation, 81: 1319-1330, 1990.

[22] Moran PR. A flow velocity zeugmatographic interlace for NMR imaging in humans. Magn Reson Imaging., 1:197–203, 1982.

[23] Morse OC, Singer JR. Blood velocity measurements in intact subjects. Science, 170: 440–441, 1970

[24] Nayler GL, Firmin DN, Longmore DB. Blood flow imaging by cine magnetic resonance. J Comput Assist Tomogr., 10:715–722, 1986.

[25] Nichols WW, O'Rourke MF. McDonald's blood flow in arteries (V Edition). Hodder Arnold Eds., 1990

[26] O'Donnell M. NMR blood flow imaging using multiecho, phase contrast sequences. Med Phys., 12:59–64, 1985.

[27] Oelhafen M, Schwitter J, Kozerke S, Luechinger R, Boesiger P. Assessing Arterial Blood Flow and Vessel Area Variations Using Real-Time Zonal Phase-Contrast MRI. . J Magn Reson Imaging., 23:422–429, 2006.

[28] Okada Y, Ono S, Takizawa T, Ishihara S, Sugiyama Y, Watanabe M, Saegusa N. Assessment of Pulmonary Artery Flow Velocity using a Doppler Guidewire after the Fontan Operation. Respiration and Circulation., 46 (12): 1223-1229, 1998.

[29] Pelc NJ, Herfkens RJ, Shimakawa A, Enzmann DR. Phase contrast cine magnetic resonance imaging. Magn Reson Q., 7:229–254, 1984.

[30] Pelc NJ, Sommer FG, Li KC, Brosnan TJ, Herfkens RJ, Enzmann DR. Quantitative magnetic resonance flow imaging. Magn Reson Q., 10:125–147, 1994.

[31] Ponzini R. Computational modelling of local haemodynamics phenomena: methods, tools and clinical applications. PhD Thesis, 2007.

[32] Ponzini R, Lemma M, Morbiducci U, Antona C, Montevecchi FM, Redaelli A. Doppler derived quantitative flow estimate in coronary artery bypass graft: a computational multiscale model for the evaluation of the current clinical procedure. Med Eng Phys., 30(7):809-16, 2008.

[33] Ponzini R, Vergara C, Redaelli A, Veneziani A. Reliable CFD-based estimation of flow rate in haemodynamics measures. Ultrasound Med Biol., 32(10):1545-55, 2006.

[34] Privat C, Ravel A, Chirossel P, Borson O, Perez N, Bourlet P, Walker L, Viallet JF, Boyer L. Endovascular Doppler guide wire in renal arteries: Correlation with angiography in 20 patients. Investigative Radiology, 34 (8): 530-535, 1999.

[35] Sambuceti G, Marzilli M, Marraccini P, Schneider-Eicke J, Gliozheni R, Parodi O, L'Abbate A. Coronary vasoconstriction during myocardial ischemia induced by rises in metabolic demand in patients with coronary artery disease. Circulation, 95(12):2652-9, 1997.

[36] Savader SJ, Lund GB, Osterman FA. Volumetric evaluation of blood flow in normal renal arteries with a Doppler flow wire: a feasibility study, Journal of Vascular and Interventional Radiology, 8(2): 209-214, 1997.

[37] Rigatelli Gia, Barbiero M, Docali G, Zanchetta M, Pedon L, Baratto A, Maiolino P, Rigatelli Gio, Carraro U, Dalla Volta S. Validation of Doppler Flow Guidewire for Peak Aortic Flow Measurement in Order to Establish Its Sensitivity for Recognition of Cardiac Assistance in Demand Dynamic Cardiomyoplasty. Basic Appl Myol., 10 (3): 127-130, 2000.

[38] Tsangaris S, Stergiopulos N. The inverse Womersley problem for pulsatile flow in straight rigid tubes. J. Biomech., 21(3): 263-266, 1998.

[39] Tsujino H, Jones M, Qin JX, Cardon LA, Morehead AJ, Travaglini A, Bauer F, Zetts AD, Greenberg NL, Panza JA, Thomas JD. Estimation of the spatial mean and peak flow velocities using real-time 3D color Doppler echography: in vitro and in vivo studies. Computers in Cardiology, 26: 173-176, 1999.

[40] Underwood SR, Firmin DN, Klipstein RH, Rees RS, Longmore DB. Magnetic resonance velocity mapping: clinical application of a new technique. Br Heart J., 57:404–412, 1987.

[41] Van Dijk P. Direct cardiac NMR imaging of heart wall and blood flow velocity. J Comput Assist Tomogr., 171:429–436, 1984.

[42] Veneziani A., Vergara C. Flow rate detective boundary conditions in haemodynamics simulations. Int. J. Num. Meth. Fluids, 47: 803-816, 2005.

[43] Vergara C, Ponzini R, Veneziani A, Redaelli A, Neglia D, Parodi O. Reliable CFD-based Estimation of Flow Rate in Hemodynamics Measures: Sensitivity Analysis and First Clinical Validation. Submitted.

[44] Walker MF, Souza SP, Dumoulin CL. Quantitative flow measurement in phase contrast MR angiography. J Comput Assist Tomogr., 12:304–313, 1988.

[45] Watanabe N, Akasaka T, Yamaura Y, Kamiyama N, Akiyama M, Koyama Y, Neishi Y, Yoshida K. Noninvasive assessment of great cardiac vein flow by Doppler echocardiography: a validation study. Journal of the American Society of Echocardiography, 15 (3): 253-258, 2002.

[46] Womersley JR. Method for the calculation of velocity, rate of flow and viscous drag in arteries when the pressure gradient is known. J. Physiol., 127(3):553-63, 1955

## Tables

| Arterial district | TR [ms] | TE [ms] | Pixel size [mm] | Slice thikness [mm] | Cardiac phases |
|---|---|---|---|---|---|
| Abdominal aorta | 30.85 | 4.05 | 0.86 | 5.0 | 30 |
| Common carotid | 83.9 | 4.79 | 0.70 | 3.0 | 20 |
| Brachial | 77.0 | 4.11 | 0.47 | 3.0 | 15 |

Table 1. PCMRI acquisition protocol: the abdominal aorta, the common carotid artery and the brachial artery have been acquired using 2D cine-PC MRI technique. For each arterial district the main MRI acquisition parameters are reported

.

**List of Figures**

performed over the all dataset and considering the flat hypothesis within the a-priori approach only for data concerning the abdominal aorta.

**Figure 7.** 3D/2D spatial velocity profiles. *a*) Abdominal aorta; *b*) Common carotid artery; *c*) Brachial artery. To get a simpler visualization of the changing of the spatial velocity profiles at different Womersley values, the 2D velocity profiles across a single (normalized) diameter in each district are shown for a single representative subject, and compared with a parabola sharing the same value of maximum velocity $V_M$ (vertex of the parabola, in cm/s). In the case of abdominal aorta (*c* panel) we report also the flat profile constructed on the same value of velocity.

**Figure 8.** Dependence of the blood flow rate on *W*. The relative errors of the estimates obtained with the *a priori* and the *Womersley-based* approaches are shown as function of the Womersley number values (left, marked with *a*). The relative errors of the estimates obtained with the *a priori* approach by using the *in vivo* dataset provided in this work and in the *in silico* validation obtained in [33], are plotted as a function of the Womersley number (right, marked with *b*).

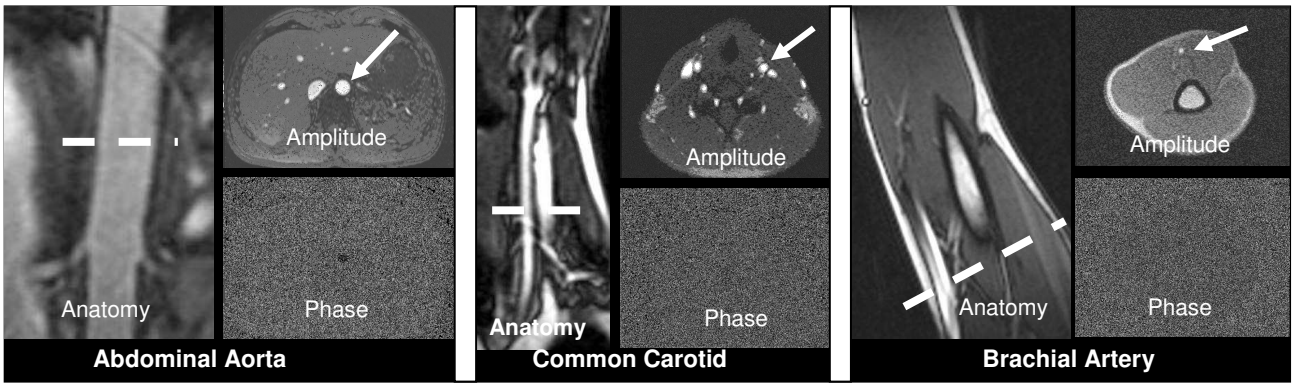
Amplitude
Anatomy
Phase
Abdominal Aorta
Amplitude
Anatomy
Phase
Common Carotid
Amplitude
Anatomy
Phase
Brachial Artery

a b c

Figure 1.

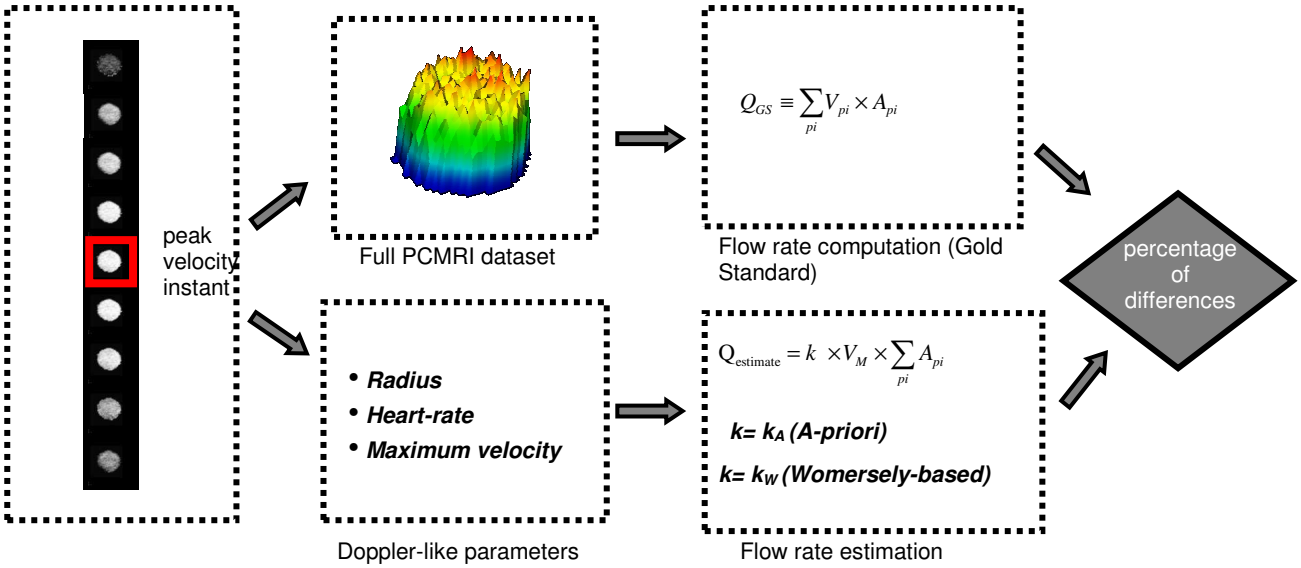
peak
velocity
instant
Full PCMRI dataset
$Q_{GS} \equiv \sum_{pi} V_{pi} \times A_{pi}$
Flow rate computation (Gold Standard)
percentage of differences
• Radius
• Heart-rate
• Maximum velocity
$Q_{estimate} = k \times V_M \times \sum_{pi} A_{pi}$
k= $k_A$ (A-priori)
k= $k_W$ (Womersely-based)
Doppler-like parameters
Flow rate estimation

Figure 2.

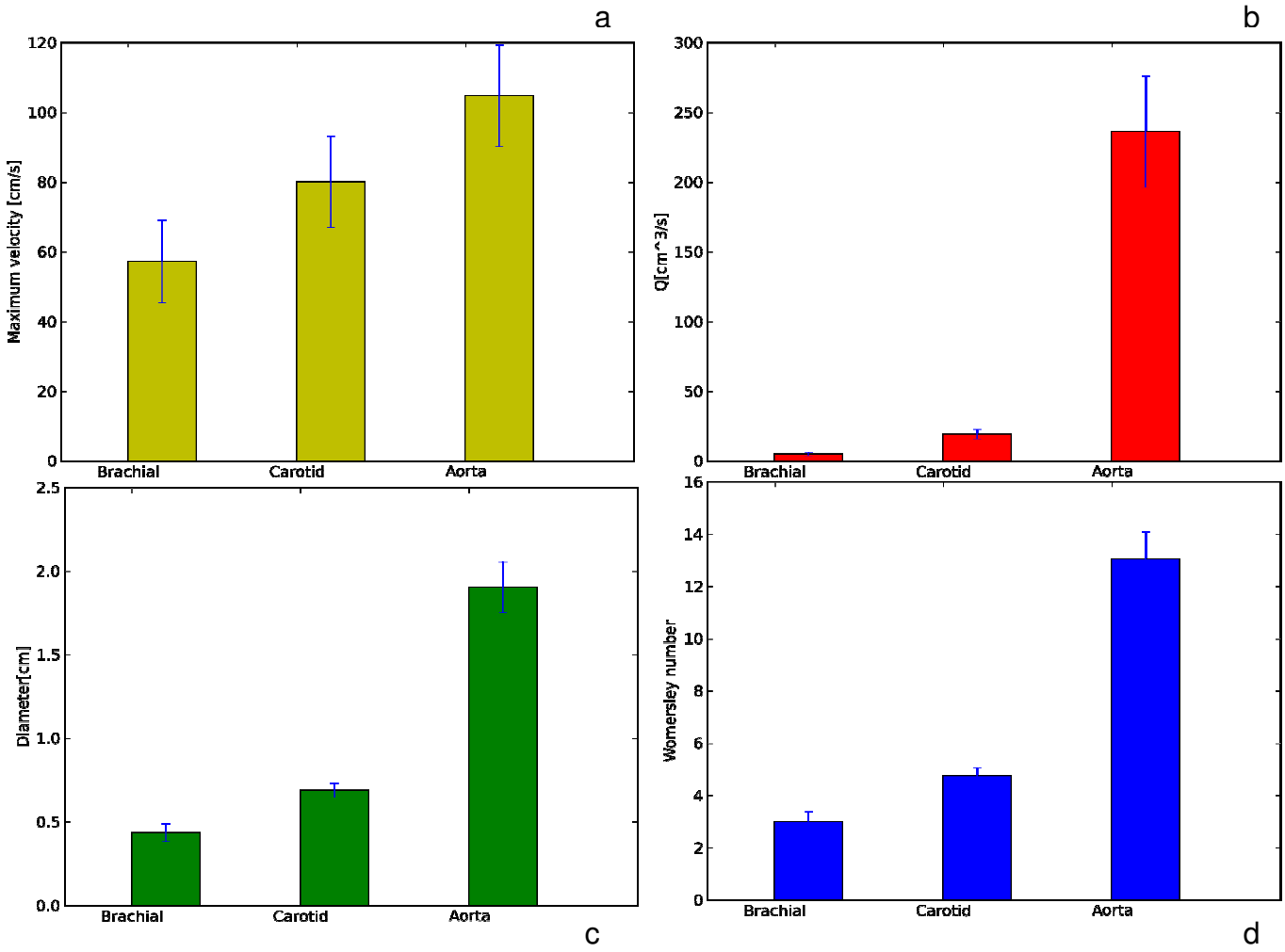
a
b
c
d
Maximum velocity [cm/s]
Q[cm^3/s]
Diameter[cm]
Womersley number
Brachial
Carotid
Aorta

Figure 3.

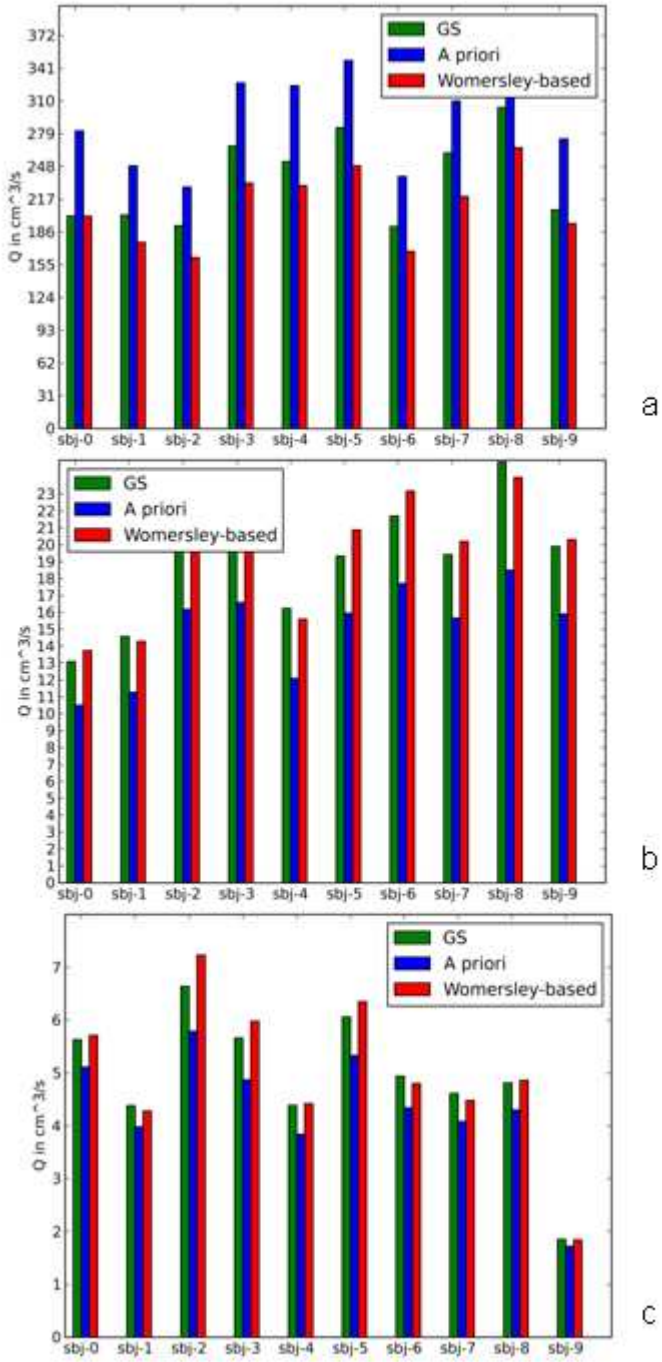
GS
A priori
Womersley-based
Q in cm^3/s
sbj-0
sbj-1
sbj-2
sbj-3
sbj-4
sbj-5
sbj-6
sbj-7
sbj-8
sbj-9
a
b
c

Figure 4.

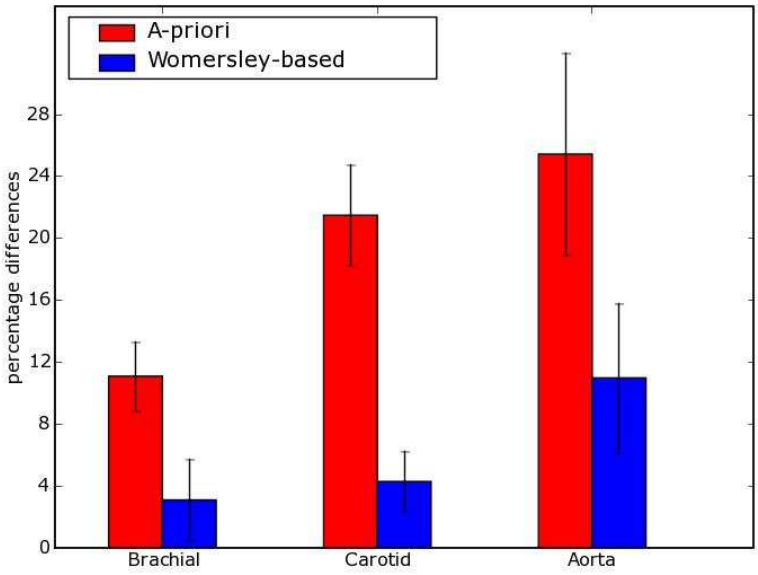
A-priori
Womersley-based
percentage differences
0
4
8
12
16
20
24
28
Brachial
Carotid
Aorta

Figure 5.

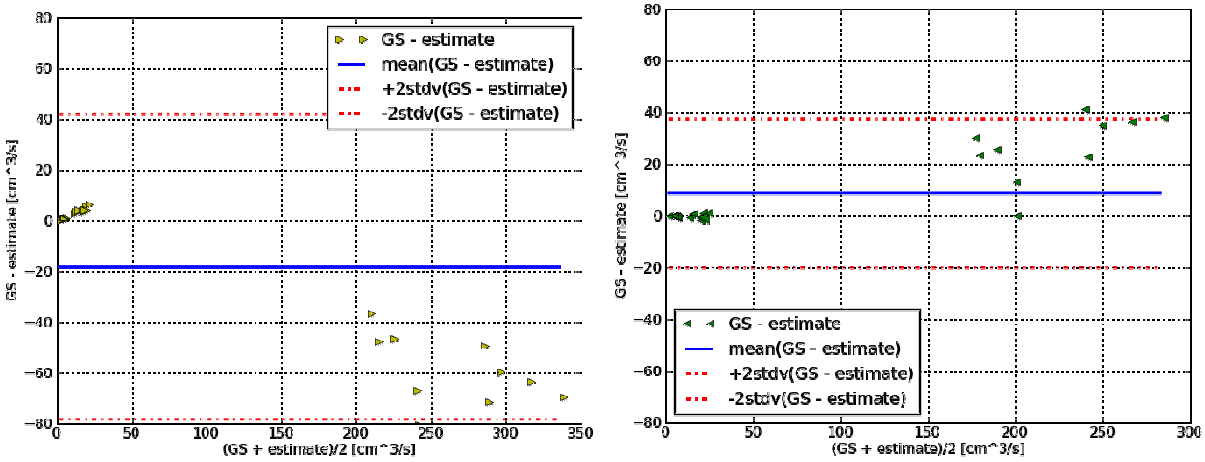
GS - estimate
mean(GS - estimate)
+2stdv(GS - estimate)
-2stdv(GS - estimate)
GS - estimate [cm^3/s]
(GS + estimate)/2 [cm^3/s]
GS - estimate
mean(GS - estimate)
+2stdv(GS - estimate)
-2stdv(GS - estimate)
GS - estimate [cm^3/s]
(GS + estimate)/2 [cm^3/s]

Figure 6.

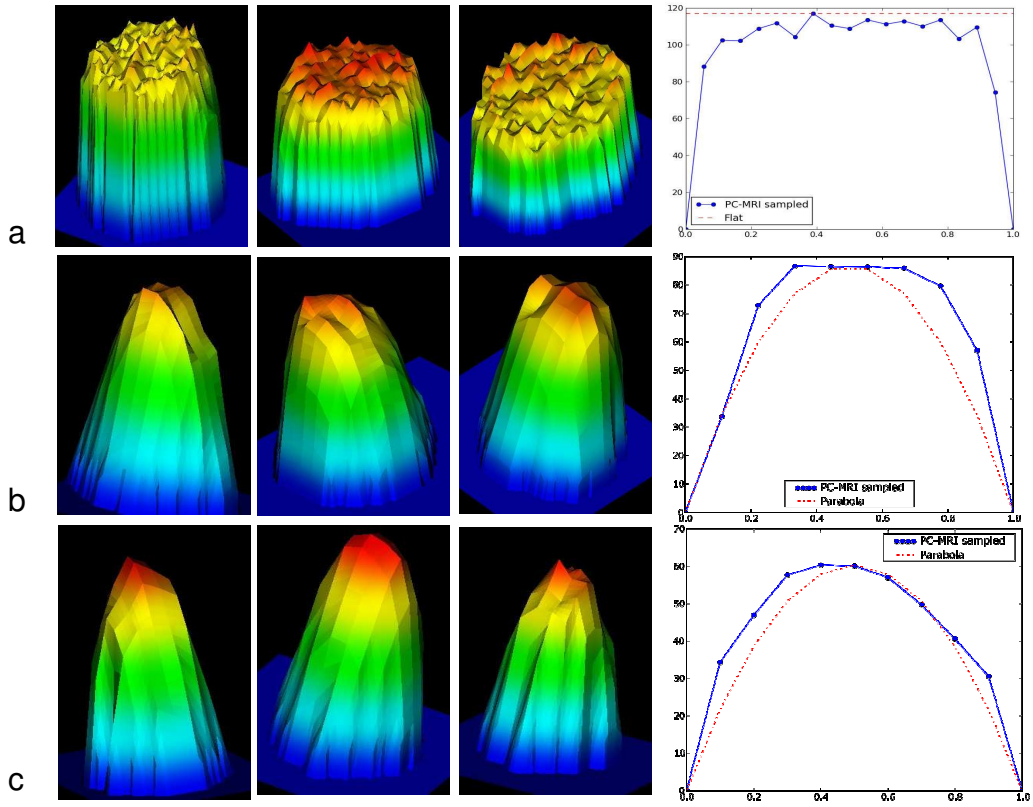
a
b
c
PC-MRI sampled
Flat
PC-MRI sampled
Parabola
PC-MRI sampled
Parabola

Figure 7.

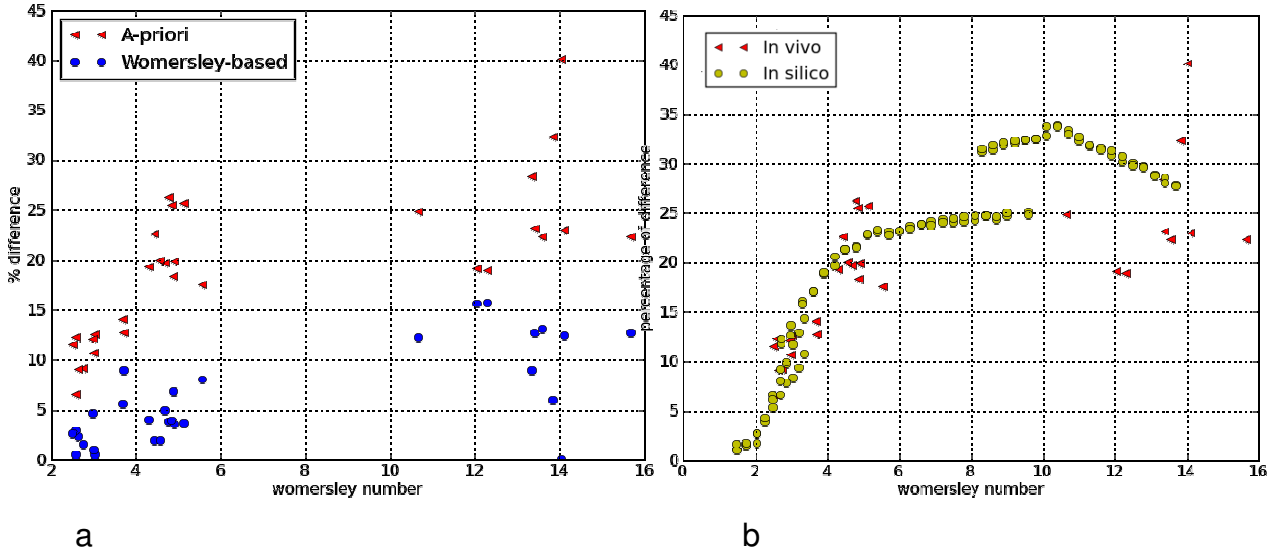
A-priori
Womersley-based
% difference
womersley number
In vivo
In silico
womersley number

a b

Figure 8.